

Intraparticle Magnetic Properties of Co_3O_4 Nanocrystals

Syozo Takada, Mikiko Fujii, and Shigemi Kohiki*

*Department of Materials Science, Kyusyu Institute of Technology,
Kita-kyusyu 804-8550, Japan*

Tomohiro Babasaki and Hiroyuki Deguchi

*Department of Electronics, Kyusyu Institute of Technology,
Kita-kyusyu 804-8550, Japan*

Masanori Mitome

*Advanced Materials Laboratory, National Institute of Materials Science,
Tsukuba 305-0044, Japan*

Masaaki Oku

Institute for Materials Research, Tohoku University, Sendai 980-8577, Japan

Received April 12, 2001; Revised Manuscript Received June 15, 2001

ABSTRACT

We have prepared a diluted system of Co_3O_4 nanocrystals dispersed in nonmagnetic SiO_2 by heating an MCM-41 molecular sieve soaked in 0.075 mol/L CoCl_2 aqueous solution in flowing oxygen at 300 °C for 3 h. Transmission electron microscopy showed that fine particles of about 3 nm exhibiting the (220) and (331) lattice fringes of the Co_3O_4 crystal distribute randomly in amorphous SiO_2 . Magnetic measurements using a SQUID magnetometer suggested the presence of quantum resonant spin tunneling of intraparticle superparamagnetic moments below the blocking temperature. The maximum points in the ac susceptibility shifted toward higher temperature from ≈ 3 to ≈ 5 K with increasing the frequency from $\approx 10^{-2}$ to $\approx 10^3$ Hz. There were no divergent peaks above 1.7 K in the nonlinear susceptibility. The field dependent magnetization from 0 to ≈ 20 kG showed a small hysteresis loop at 2 K, whereas there were no hysteresis loops at both 5 and 10 K. The diluted Co_3O_4 nanocrystals is a new and ideally suitable material for the study of macroscopic magnetic quantum effects.

Macroscopic quantum tunneling of magnetization, reported for the Mn_{12} acetate,^{1–5} the horse spleen ferritin,^{6–12} and so on,^{13,14} has been a subject of great interest.¹⁵ A diluted system of single domain antiferromagnetic nanocrystals with nonmagnetic medium is ideally suited to observe clearly the intraparticle macroscopic quantum tunneling phenomena,^{16,17} since the system can exclude influences of interparticle dipole interactions such as the spin glass behavior. The exponential dependence of the magnetization relaxation time on volume has spurred intensive studies of ferromagnetic nanocrystal synthesis for magnetic storage purposes.^{18,19} However, it is of great interest to prepare assemblies of single domain antiferromagnetic nanocrystals exhibiting only the intraparticle characteristics reflecting the effects of magnetically uniform size distribution and of dilution with a nonmagnetic medium. We have prepared an assembly of Co_3O_4 nanocrystals about 3 nm in diameter dispersed in the MCM-41

molecular sieve. The assembly demonstrated the magnetic response of independent particles. The diluted Co_3O_4 nanocrystals showed the thermally assisted resonant tunneling-like behavior between up- and down-spin states with a weak dissipation.

The MCM-41 molecular sieve with uniform columnar and periodic hexagonal mesopores was used as a fabrication template of the diluted Co_3O_4 nanocrystals. The MCM-41 mesoporous silicate was synthesized from a mixture of amorphous SiO_2 1.00: $\text{C}_{12}\text{H}_{25}\text{N}(\text{CH}_3)_3\text{Cl}$ 0.70: NaOH 0.24: H_2O 53.7 in molar ratio. The mixture was stirred at room temperature and then heated at 140 °C for 48 h. After thermal dehydration, the dried mixture was calcinated at 700 °C for 6 h in air. As shown in Figure 1, in X-ray diffraction (XD) measurements, the silicate sample showed that two peaks can be indexed on a hexagonal unit cell with $a \sim 4.3$ nm ($a = 2d_{100}/\sqrt{3}$ and $d_{100} = 3.7$ nm) in the region of $2\theta < 6^\circ$ ($\text{Cu K}\alpha$ radiation). The silicate sample was soaked in 0.075 mol/L CoCl_2 aqueous solution. The soaked sample was dried

* Corresponding author. E-mail: kohiki@che.kyutech.ac.jp.

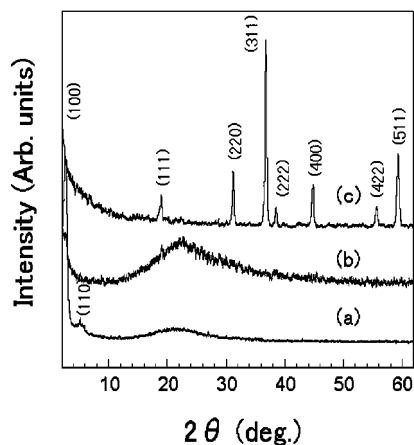


Figure 1. XRD patterns of the silicate sample (a), the heated sample (b), and the bulk Co_3O_4 powders (c). The Co_3O_4 powders used as a reference were synthesized from dried powders of the precursor solution by calcination at 750 °C for 3 h in flowing oxygen.

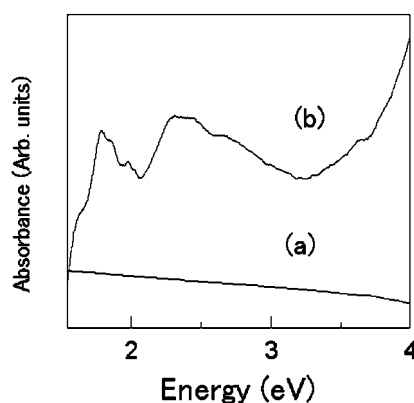


Figure 2. UV-vis diffuse reflectance spectra of the silicate sample (a) and the heated sample (b).

and then heated in flowing oxygen at 300 °C for 3 h. The XRD pattern of the heated sample suggests that the sample is amorphous and contains no crystals of both metallic Co and CoO. A smeared and small peak was found at the diffraction angle ($2\theta \approx 19^\circ$) corresponding to the Co_3O_4 (111) reflection, though it is hard to manifest the formation of Co_3O_4 nanocrystals since the peak is burying in the diffuse scattering background. As shown in Figure 2, in the ultraviolet-visible (UV-vis) optical absorption measurement the silicate sample showed no absorption peaks below 4 eV, although the heated sample exhibited both a clear absorption with triple-peaked structure at around 1.9 eV (typical for Co^{II} in tetrahedral coordination) and a broad absorption with two-peaked structure in the vicinity of 2.5 eV (typical for Co^{III} in octahedral coordination).²⁰ A representative image of high-resolution transmission electron microscopy (HRTEM) for the heated sample demonstrated that fine particles with an average size of about 3 nm distributed randomly in amorphous SiO_2 matrix. They exhibit clearly resolved lattice fringes with the interplanar spacings of 0.29 and 0.18 nm assigned to the (220) and (331) planes of the Co_3O_4 crystal, respectively (Figure 3). The sample contained about 1 mol

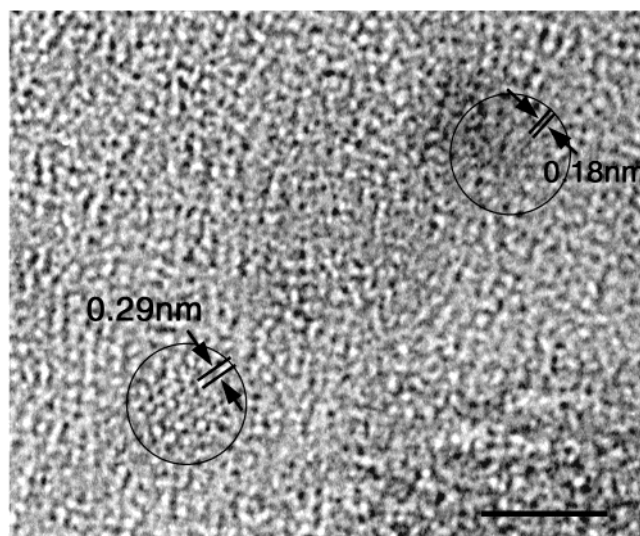


Figure 3. HRTEM (JEOL JEM-3000F) images of the diluted Co_3O_4 nanocrystals. Uncertainties exist in the measurement of the particle size due to fuzzy particle boundary. The bar corresponds to 3 nm.

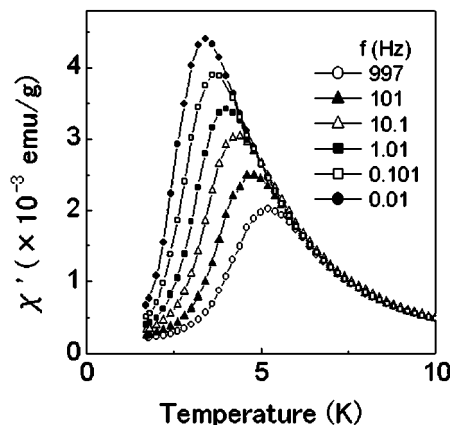


Figure 4. Frequency dependences of the χ' from $f = 0.01$ to 997 Hz in $H = 2$ G.

% Co_3O_4 . Consequently, the diluted system of Co_3O_4 nanocrystals with nonmagnetic SiO_2 was prepared successfully.

A Quantum Design MPMS 5S SQUID magnetometer was used for the susceptibility and magnetization measurements. A cooling history (zero field cooled and field cooled) dependence of the dc susceptibility was observed below 7.5 K in a magnetic field of $H = 2$ G. A sharp maximum in the zero field cooled susceptibility appeared at around 3.4 K and is expected to correspond to the freezing temperature of residual spin moments. At the freezing temperature, magnetic dipoles in a finite field cannot follow the ac external field, therefore the imaginary part should appear in the ac susceptibility. The frequency and temperature dependences of the ac susceptibility are shown in Figure 4. The peak is composed with a single component for each frequency. The ac susceptibility suggests that the size of the Co_3O_4 nanocrystals dispersed in nonmagnetic SiO_2 is magnetically uniform. Similar to the case of ferritin,^{12,21} as the frequency increased, the maximum points of both the χ' (real part) and

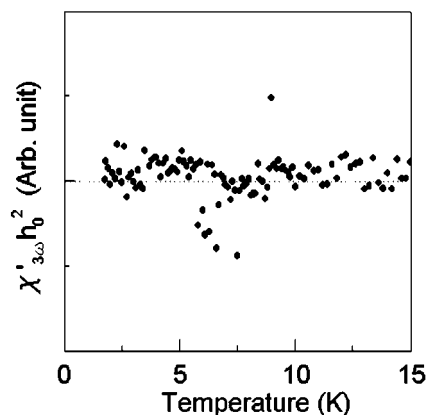


Figure 5. Temperature dependence of the χ'_3 at $f = 10$ Hz with $h_0 = 2$ G above 1.7 K.

χ'' (imaginary part) curves shifted to higher temperature with decreasing the maximum values of χ' and χ'' . The maximum temperatures at the frequency of 0.01 and 997 Hz were respectively 3.4 and 5.2 K for χ' , and were respectively 2.6 and 4.4 K for χ'' . The maximum of the $\chi(T)$ curve determines the blocking temperature (T_b), reflecting slow dynamics of the superparamagnetic moments. The rate at which individual moments of the nanocrystals jump across the anisotropy barrier U is proportional to the Arrhenius factor, $\exp(-U/T)$. At low T , the total magnetization M in the direction of H is rather small, since the all moments of the nanocrystals are frozen. As the T goes up, the nanocrystals unfreeze their moments and the M along H increases. Above the T_b , moments of most of the nanocrystals are unfrozen and $\chi(T)$ approaches Curie's law. As it is expected, both the $T_b(\chi')$ and $T_b(\chi'')$ increased as the f of H increased. To estimate the U' and U'' values, these frequency dependences were fitted to the equation $T_b = U/k_B \ln(1/\tau_0 f)$ with the attempt time $\tau_0 = 1 \times 10^{-12}$ s. Here, k_B is the Boltzmann constant. The fitted values of U'/k_B and U''/k_B were approximately 110 and 90 K, respectively. Writing $U = KV$, where K is the energy density of the magnetic anisotropy and V is the volume of the nanocrystals, we find that at $T_b = 3$ K the Co_3O_4 nanocrystals of the diameter 3 nm have $K = 9 \times 10^5$ erg/cm³. The order of the value for the Co_3O_4 nanocrystals is the same as that for antiferromagnetic horse spleen ferritin ($K = 2.5 \times 10^5$ erg/cm³),¹² though the value is smaller than that of ferrimagnetic CoFe_2O_4 nanocrystals of 2.5-nm diameter (8×10^6 erg/cm³).²²

Frequency dependence can be understood as an indication of a superparamagnetic or spin glass material.²³ It is well-known that a spin glass phase can be specified by the nonlinear susceptibility χ_3 . The magnetization m is expressed as $m = \chi_1 h + \chi_3 h^3 + \chi_5 h^5 + \dots$, when the applied ac field $h = h_0 \sin(\omega t)$ is so small. Here, χ_1 is the linear susceptibility and χ_3 and χ_5 are the nonlinear susceptibilities. The 3ω component can be given by $M_{3\omega} = -(1/4)\chi_3 h_0^3 - (5/16)\chi_5 h_0^5 - (21/64)\chi_7 h_0^7 + \dots$. Therefore, the real part χ'_3 is given as $\chi'_3 = -4M'_{3\omega}/h_0^3$ and is proportional to higher harmonic signals of frequency 3ω . As shown in Figure 5, the temperature dependence of the nonlinear susceptibility χ'_3 (3ω signal) showed no divergent peaks above 1.7 K. The

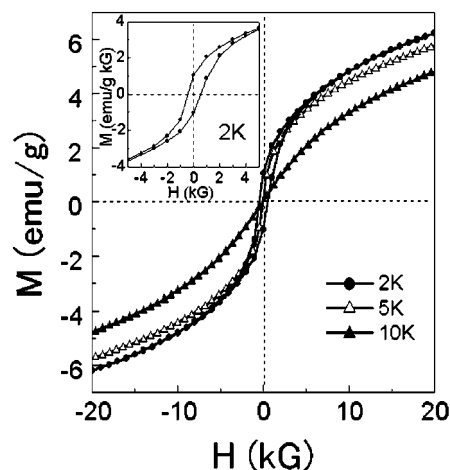


Figure 6. Field dependences of the dc magnetization measured at 2, 5, and 10 K.

nonlinear susceptibility measurement revealed that the sample is superparamagnetic and both the observed temperature and frequency dependences are due to blocking effects of the resultant spins from the uncompensation for the Co_3O_4 nanocrystals.

Fitting to the Langevin equation of the field-dependent magnetization measured at 20 K gave about five uncompensated Co^{II} ions, which agreed well with the estimated surface ions (approximately six) for the Co_3O_4 nanocrystals of 3 nm diameter containing ≈ 240 Co^{II} ions.^{24,25} Such a low moment means that the magnetic dipole interaction between the nanocrystals is negligibly small, and it is an independent proof of the single-particle nature of the effect due to superparamagnetic moments. Both the measurements of nonlinear susceptibility and field-dependent magnetization imply that in this experiment modification of U by the magnetic dipole interactions between different nanocrystals can be neglected and the system is in the superparamagnetic state.

Near the T_b , there is always a faster relaxation of the total magnetization associated with the superparamagnetic behavior of the major part of the particles. We found a small hysteresis loop on the magnetization curve measured at 2 K ($< T_b$), although both the magnetization curves measured at 5 K ($\approx T_b$) and 10 K ($> T_b$) showed no hysteresis loops, as shown in Figure 6. Anomaly near zero field is more apparent for the 5 K curve than the 10 K one. The field derivative of the magnetization curve (dM/dH) method has been used to detect the resonant spin tunneling in Mn_{12} acetate and ferritin.¹⁰ As expected from such a weak dissipation, dM/dH (the figure is not shown) for 2 K showed twin peaks reversible with the field near $H = 0$, and those for 5 and 10 K showed a quite sharp peak and a dull peak at $H = 0$, respectively. The result is very similar to the cases of Mn_{12} acetate and ferritin. The magnetic relaxation rate was drastically enhanced as the field approaches zero at lower temperature, though the enhancement was larger for 5 K ($\approx T_b$) than for 2 K ($< T_b$). A possible interpretation is as follows. Thermal process is essentially frozen below T_b , and the transition between up- and down-spin states occurs only

via resonance quantum tunneling. Below T_b , the spin levels in the potential wells separated by U should match to provide a high tunneling rate corresponding to the resonant spin tunneling. However, the M along H at 2 K is rather smaller than that at 5 K because of the blocking of the superparamagnetic moments. Therefore, the observed enhancement in the magnetic relaxation at 2 K became rather smaller than that at 5 K. Larger enhancement for 5 K, resulted from greater M of unfrozen dipole moments, implies that the potential wells have essentially the same energy, even at 5 K. At 10 K, the relaxation was dominated by off-resonance tunneling and the rate became so small.

Finally, the diluted Co_3O_4 nanocrystals showing the intrinsic nature of single domain antiferromagnetic fine particles were synthesized chemically by only heating at 300 °C the mesoporous silicate soaked to the precursor solution.

Acknowledgment. S.T. is grateful to the Sasakawa Scientific Research Grant from The Japan Science Society for supporting the present work. S.K. thanks the support of the Corning Japan Research Grant for this work. A part of this work performed under the interuniversity cooperate research program of Laboratory for Advanced Materials, the Institute for Materials Research, Tohoku University.

References

- (1) Friedman, J. R. et al. *Phys. Rev. Lett.* **1996**, 76, 3830.
- (2) Sessoli, R. et al. *Nature* **1993**, 365, 141.

- (3) Thomas, L. et al. *Nature* **1996**, 383, 145.
- (4) Garanin, D. A.; Chudonovsky, E. M. *Phys. Rev. B* **1997**, 56, 11102.
- (5) Pohjola, T.; Schoeller, H. *Phys. Rev. B* **2000**, 62, 15026, and references therein.
- (6) Awachalom, D. D.; DiVincenzo, D. P.; Smyth, J. *Science* **1992**, 258, 414.
- (7) Awachalom, D. D. et al. *Phys. Rev. Lett.* **1992**, 68, 3092.
- (8) Tejada, J.; Zhang, X. X. *J. Phys.: Condens. Matter* **1994**, 6, 263.
- (9) Gider, S. et al. *J. Appl. Phys.* **1996**, 79, 5324.
- (10) Tejada, J. et al. *Phys. Rev. Lett.* **1997**, 79, 1754.
- (11) Friedman, J. R.; Voskoboynik, U.; Sarachik, M. P. *Phys. Rev. B* **1997**, 56, 10793.
- (12) Luis, F. et al. *Phys. Rev. B* **1999**, 59, 11837.
- (13) Taft, K. L. et al. *J. Am. Chem. Soc.* **1994**, 116, 823.
- (14) Wernsdorfer, W.; Sessoli, R. et al. *Science* **1999**, 284, 133.
- (15) Chudonovsky, E. M.; Tejada, J. *Macroscopic Quantum Tunneling of Magnetic Moment*; Cambridge University Press: Cambridge, 1998.
- (16) Barbara, B.; Chudonovsky, E. M. *Phys. Lett. A* **1990**, 145, 205.
- (17) Lu, R. et al. *Eur. Phys. J. B* **2000**, 14, 349.
- (18) Thurn-Albrecht, T. et al. *Science* **2000**, 290, 2126.
- (19) Puentes, V. F.; Krishnan, K. M.; Alivisatos, A. P. *Science* **2001**, 291, 2115.
- (20) Figgis, B. N. *Introduction to Ligand Fields*; Interscience: New York, London, Sydney, 1966.
- (21) Kilcoyne, S. H.; Cywinski, R. *J. Magn. Magn. Mater.* **1995**, 140–144, 1466.
- (22) Chudonovsky, E. M.; Tejada, J. *Macroscopic Quantum Tunneling of Magnetic Moment*; Cambridge University Press: Cambridge, 1998; p 123.
- (23) Mulder, C. A.; van Duynveldt, A. J.; Mydosh, J. A. *Phys. Rev. B* **1981**, 23, 1384.
- (24) Dormann, J. L.; Fiorani, D.; Tronc, E. *Adv. Chem. Phys.* **1977**, 98, 283.
- (25) Kundig, W. et al. *J. Phys. Chem. Solids* **1969**, 30, 819.

NL015538X